Analysis of charged particle multiplicity data.
Some thoughts and comments based on event generator data.

Jens Jørgen Gaardhøje.

Sept. 2000.09.28
BRAHMS analysis note.

1 What is this about?

The present document is meant as a small contribution to the analysis of charged particle multiplicity data from BRAHMS and in particular the assessment of correction factors and systematic errors. Herein we (pluralis majestaeticus) analyze simulated data from the NEXUS and HIJING event generators.

Based on the (rough) knowledge of the positions and dimensions of the various detector elements we can simulate particle spectra, multiplicity distributions etc. in different detectors and investigate various trigger or physics constraints. For the analysis of energy loss spectra we use the Bethe-Bloch formula assuming a density for plastic of $1.03g/cm^3$ (see Bicron spec. sheets) and equal numbers of H and C atoms (thus Aeff=6.5 ,Zeff=3.5).

We have investigated the following issues, which are briefly described in this note:

- Procedures for determining the charged particle multiplicity in the Plastic Tile Multiplicity Array including an assesment of systematic errors from analysis of total energy loss spectra.
- Estimated $dN/d\eta$ distributions for charged particles (π, K, p of both signs) vs. centrality for the 2 considered models.

Obviously, this analysis is not meant to provide highly accurate numbers, nor can it address the issue of background contributions from the production of secondary particles etc. Nevertheless we find it useful as it allows to retrace the analysis procedure in some detail and compare to known answers.

We hope that this note will stimulate the discussion on how to analyze the data now and in the future

2 Simulation of the PTMA analysis.

The PTMA array is described as a tube enclosing the beam pipe. Each tile is 12 cm wide and placed at 15 cm (is this correct?) from the beam pipe. There are 8 tiles sections along the z direction numbered from 1 to 8. The nominal vertex is between tiles 4 and 5. We have not bothered to simulate quadratic slats tangent to this tube. This will underpredict the spread in energy losses a little bit, but this is a minor effect. The advantage is that we use the full statistics over a 2π range in ϕ.

We analyze a NEXUS calculation for Au+Au at $\sqrt{s} = 130AGeV$. There are 500 events with impact parameters b=0-15 fm. The calculation allows all resonances to decay and should thus be appropriate for simulating the experiment. We have also looked at a HIJING calculation for $\sqrt{s} = 130GeV.A$ and b=5fm , found at BNL (100 events). The details of the control parameters for the calculation are not known! Does anybody know?

We concentrate on two PTMA elements called 1 and 4 covering pseudorapidity intervals 0-0.7 and 1.61-1.88 respectively. This may not be a fully correct description of the experimental conditions, but is adequate for the purpose of this investigation.

2.1 Analysis of particles from collisions.

2.1.1 General considerations on method.

The experimental determination of the charged particle multiplicity in the PTMA and the BB relies on the measurement of the total energy deposited per event, Etot. The number of particles in each event is then determined from

$$Npart = Etot / < Epart >,$$

where $< Epart >$ is the average energy deposited per event. Sources of errors are 1) unwanted contributions to Etot from background and random reactions, secondaries etc. and 2) incorrect determination of $< Epart >$.

The situation is exemplified in fig. 1. The two leftmost panels in the upper row show the energy loss of the charged particles from the reaction that pass through PTMA1 and PTMA4 (HIJING calculation for $\sqrt{s} = 130GeV.A$ and b=5fm). The energy loss has been calculated simply by looking up the dE/dx predicted by the Bethe-Bloch formula at the $\beta\gamma$ value of the considered particle. For each particle, the polar angle is calculated and the effective energy loss (dE) through the detector is calculated (factor $1/sin(\theta)$). The two leftmost panels in the lower row show the corresponding calculated distributions of $\beta\gamma$ vs. dE .

The two energy loss spectra show peaks of different widths and also significant tails. The peaks are clearly associated with fast moving particles and the tails are associated with slow moving more ionizing particles. The width of the peak arises from the finite bite in polar angle subtended by each slat leading in a spread of energy losses. Note that the effect of 'corners' in the Tiles is not properly included. Thus theres are no very small energy losses. (From GEANT we see that this contributes with about 10% of the peak in PTMA1, but only about 2% in PTMA4) at large pseudorapidity. The tail contributes most for the PTMA4 detector which is closest to midrapidity since the laboratory momentum of particles in the lowest here. The fraction of tail to total is 11% above 2 MeV for PTMA4 but only 2.5% above 5.5 MeV for PTMA1 (considered range dE=0-15 MeV). Most of the tail is due to the contribution from slow moving pion (low pt) since these constitute the bulk of the produced particles. This is easily verified by setting a low-pt threshold (f.x. 50 or 100 MeV).

For each event the individual energy losses are summed to produce the calculated

$$Etot = \sum_i dE_i$$

distribution. This is shown in the rightmost panel in the upper row (blue histogram).

The number of particles can now be estimated by dividing Etot on an event-by-event basis by the average energy loss. Two approaches can be considered: 1) use the average energy deposited by a minimum ionizing particle or 2) use the average of the dE distribution.

Method 1 implies that one starts from the measured 1 MIP response to particles of well defined momentum (monochromatic electrons or cosmic rays, say). The contribution from the tail must then be estimated from a simulation and the number of particles corrected by some factor. Method 2 is really equivalent since it also requires the use of simulations and amounts to rescaling known 1 MIP energies to make them agree with the average of the dE spectrum, which has tails. The only way to avoid this is to measure the effective 1 particle response, determined as the average of the measured dE spectrum for events in which only 1 particle passed through the detector (f.ex. events validated by tracks in a TPC).

In any case it is instructive to estimate the error that follows from these procedures.

2.1.2 Calculating Npart from average MIP energy.

The lower rightmost panel shows the mistake made in estimating the number of particles in PTMA4 (in percent) by dividing the total energy recorded in the tile, in each event, by an average MIP energy. Concretely, the plot shows the distribution of

$$\frac{Etot/ < Epart > -Npart(model)}{Npart(model)} * 100.$$

If we for $< Epart >$ use the average MIP energy (defined as the average of the energy loss of particles with $\beta\gamma > 1$, i.e. 1.39 MeV for PTMA4 and $\beta\gamma > 1.5$, i.e. 3.88 MeV for PTMA1) we overestimate the number of particles by 20.6% for PTMA4, but only by 6.7% for PTMA1. This reflects that the amount of high energy tail is relatively smaller in detectors at high pseudorapidities as compared to detectors located at small pseudorapidities (primary particles have higher momenta).

The upper right panel in fig. 1. also shows in green color the overlaid histogram of the Etot distribution obtained by only including in the sum particles with $\beta\gamma > 1$ in the case of PTMA4, i.e selecting particles in the 'MIP-band'. The resulting distribution Etot has a lower mean value and a narrower width. This selection criterium means rejecting approximately 20% of the particles.

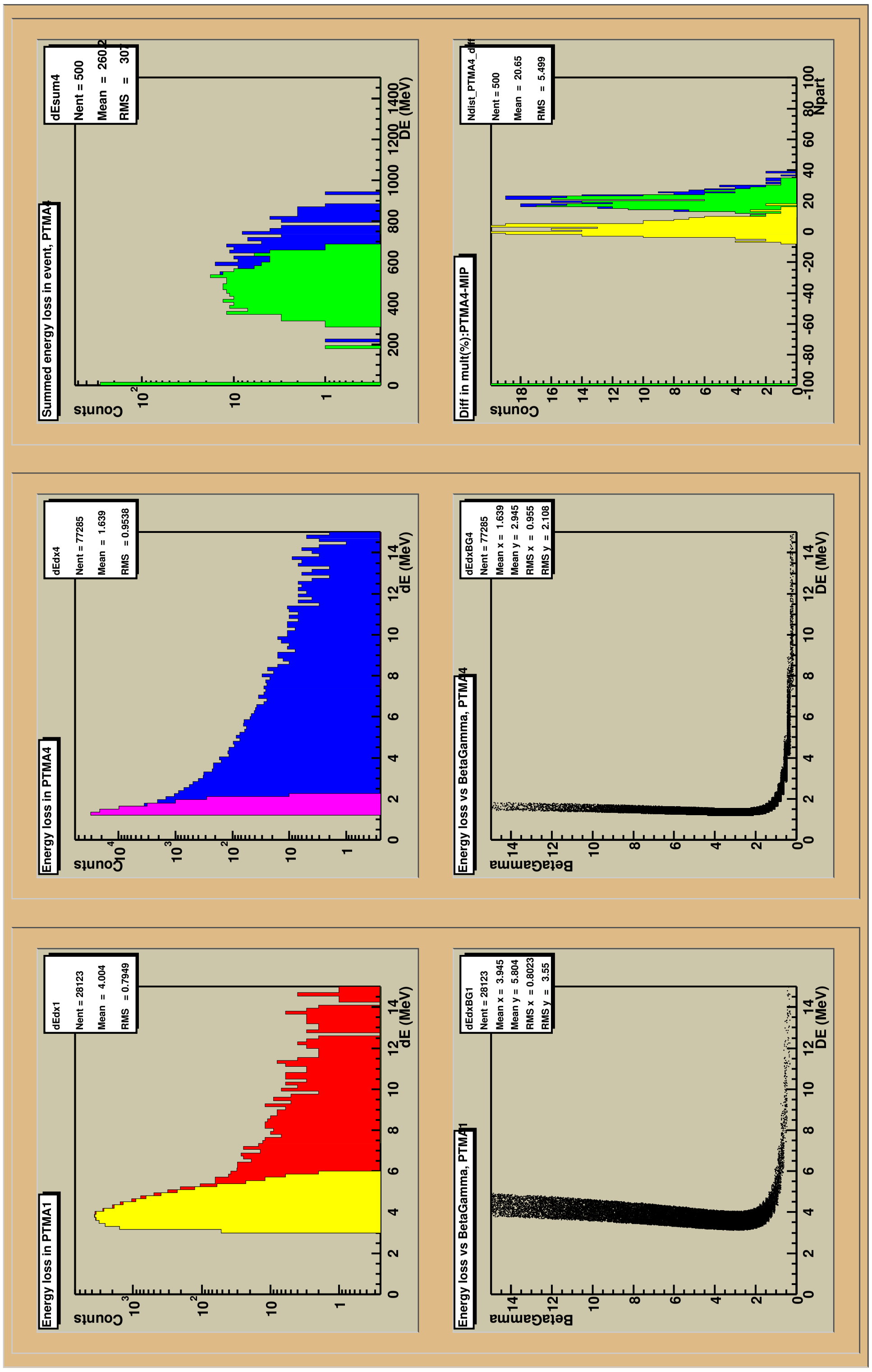

Figur 1: Upper row. Left and middle: dE spectra for PTMA1 and 4 respect. Right: Etot spectra for PTMA4 constructed from all dE (blue) and for $dE < 2.5 MeV$ (green). Lower row. left and middle: energy loss spectra vs. betagamma. Right: Difference in percent between number of calculated and real number of particles from the blue and green Etot spectra in upper row and using the average energy loss (yellow)spectra. Input: Hijing calculation at 130AGeV for b= 5fm.

The procedure illustrates that a decision must be made in deciding what an average MIP energy is, in particular if we, for this value, rely on f. ex. cosmic rays measured in a test setup.

2.1.3 Trimming the upper edge of Etot.

It is interesting to consider what happens if we 'trim' the upper edge of the Etot distribution before calculating Npart. We might naively expect that the difference between the 'real' number of particles, and the' experimentally determined' number of particles would be smaller. This is NOT the case (see green overlay in the bottom right panel as compared to blue).The difference between the two scenarios is at most a percent.The yellow peak shows the similar difference obtained using the average dE.

This implies that the large total pulse heights do NOT normally arise from the accumulation of many highly ionizing particles in a single event and a single tile. Rather, the large Etot values reflect mostly fluctuations in the multiplicity and particle composition in an event by event basis. Thus we should be careful in not trimming this tail 'ad hoc', as we will loose potential physics, not least when we start looking in more details at multiplicity fluctuations.

2.1.4 Calculating Npart from the average of the energy loss distribution.

The second method relies upon dividing the Etot determined in each event by the average of the energy loss of charged particles. Unless individual particles are resolved, we must rely on simulations to obtain this number.

In the case of HIJING events (b=5) the average energy loss is 1.643 MeV in PTMA4, and 3.882 MeV in PTMA1, determined over the energy loss range 0-15 MeV . Using these numbers we find that the difference between the 'real' number of particles and the 'calculated' number is about $1.62 \pm 0.60\%$ for PTMA4 ($\sigma = 4.88 \pm 0.56\%$) and $0.64 \pm 0.34\%$ for PTMA1 ($\sigma = 2.08 \pm 0.27\%$). See yellow distribution in fig. 1 lower right.

Note that the difference in estimated number of particles by the two methods agrees roughly (within a few percent) with the difference in average particle energies that are used (and as would be expected).

2.1.5 Other models.

There is some small dependence of these numbers on the chosen event generator, although most is partly masked by the statistical errors due to the finite number of events and particles considered.

Using as input a NEXUS calculation for $65A.GeV + 65A.GeV$ (b=0-5 fm) we find that the average energy loss is 1.652 MeV in PTMA4, and 3.969 MeV in PTMA1, determined over the energy loss range 0-15 MeV. Using these numbers we find that the difference between the 'real' number of particles and the 'calculated' number is about $3.00 \pm 1.2\%$ for PTMA4 ($\sigma = 5.7 \pm 1.40\%$) and $-0.55 \pm 0.20\%$ for PTMA1 ($\sigma = 1.41 \pm 0.16\%$).

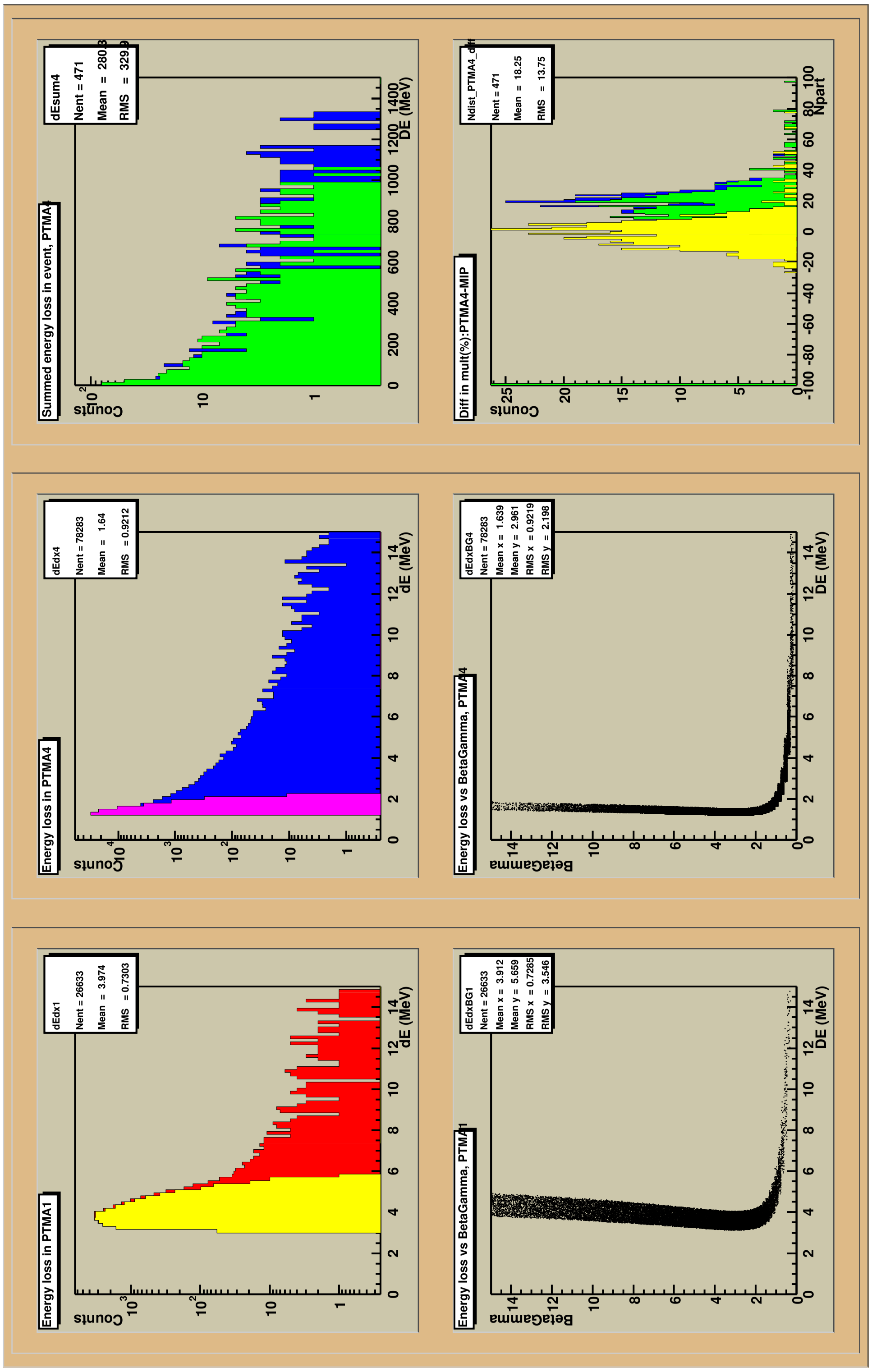

Figur 2: Same as fig 1 taking a Nexus calculation for 130AGev (b=0-15fm) as input.

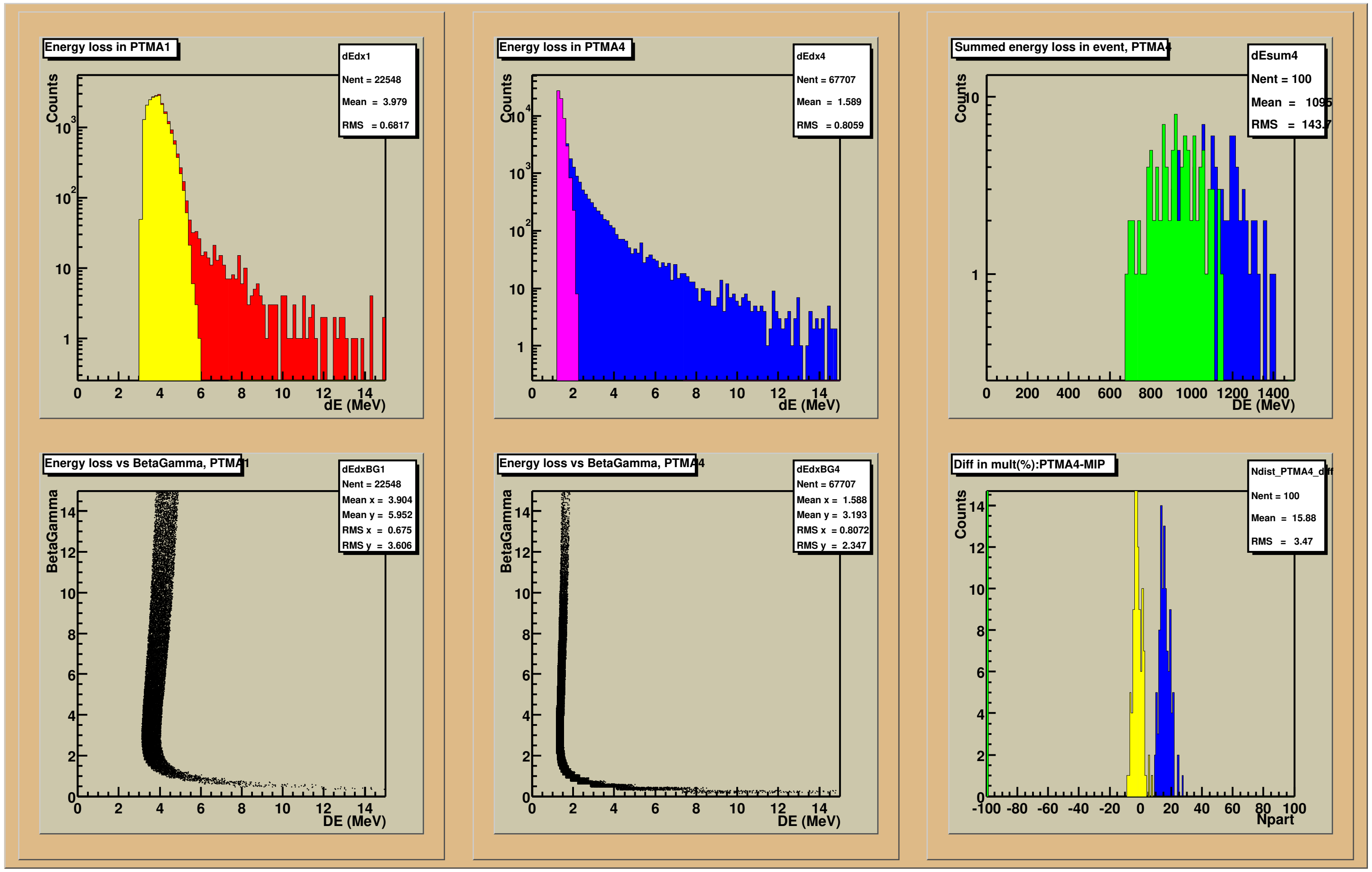

Figur 3: Same as fig 1 taking a Nexus calculation for 200AGev (b=0-2fm) as input.

Correspondingly, $< Epart >$, the average MIP energy changes little. It is defined as the average of the energy loss of particles with $\beta\gamma > 1$ for PTMA4 and is 1.406 MeV, and of particles with $\beta\gamma > 1.5$, for PTMA1 for which it is 3.864 MeV. Using these numbers we overestimate the number of particles by 21.15 % for PTMA4, but only by 2.47 % for PTMA1.

With NEXUS at higher energy (fig.3), i.e. $100A.GeV + 100A.GeV$ and b=0-2 fm we find that the average energy loss is 1.589 MeV in PTMA4, and 3.979 MeV in PTMA1, determined over the energy loss range 0-15 MeV . The difference between the 'real' number of particles and the 'calculated' number is about $2.00 \pm 0.31\%$ for PTMA4 (distribution with $\sigma = 2.70 \pm 0.27\%$) and $-0.27 \pm 0.22\%$ for PTMA1 (distribution width $\sigma = 1.27 \pm 0.22\%$).

The average MIP energy, still defined as the average of the energy loss of particles with $\beta\gamma > 1$, is 1.398 MeV for PTMA4 and for $\beta\gamma > 1.5$, is 3.903 MeV for PTMA1. Using these numbers we overestimate the number of particles by 16.0% for PTMA4, but only by 2.8 % for PTMA1.

In summary, the dependence on the models contributes with an uncertainty of less than 5% in the number of estimated particles on the average when using an average MIP energy. Using the average of the dE spectrum the variation in estimated number of particles is less than 2% for PTMA4 and about 1% for PTMA1. There is nevertheless also a contribution from the width of the difference spectra. This is typically of the order of 5 %. In summary, we conclude that the error on the estimates of particles using various models as input is less than 10%.

2.1.6 Effect of Collision centrality.

We have also explored the influence of varying collision centrality using a NEXUS calculation at $\sqrt{s} = 130 GeV.A$.

For b= 5-10 fm we find we find that the average energy loss is 1.634 MeV in PTMA4, and 3.975 MeV in PTMA1, determined over the energy loss range 0-15 MeV . The difference between the 'real' number of particles and the 'calculated' number is about $1.16 \pm 0.30\%$ for PTMA4 (distribution with $\sigma = 7.00 \pm 0.92\%$) and $-0.15 \pm 0.23\%$ for PTMA1 (distribution width $\sigma = 2.70 \pm 0.26\%$). The average MIP energy is 1.530 MeV for PTMA4 and 3.975 MeV for PTMA1. Using these numbers we overestimate the number of particles by 17.0% for PTMA4, but only by 2.5 % for PTMA1.

For b= 10 - 15 fm the average energy loss is 1.613 MeV in PTMA4, and 3.992 MeV in PTMA1, determined over the energy loss range 0-15 MeV . The difference between the 'real' number of particles and the 'calculated' number is about 5.4% for PTMA4 ($\sigma = 10.2$) and -1.5% for PTMA1 ($\sigma = 4.6\%$).

The average MIP energy is 1.396 MeV for PTMA4 and 3.906 MeV for PTMA1. Using these numbers we overestimate the number of particles by 11.2% for PTMA4, but only by 1.2 % for PTMA1.

Thus the conclusion is that there is no major dependence on the centrality, at least to the 5% level.

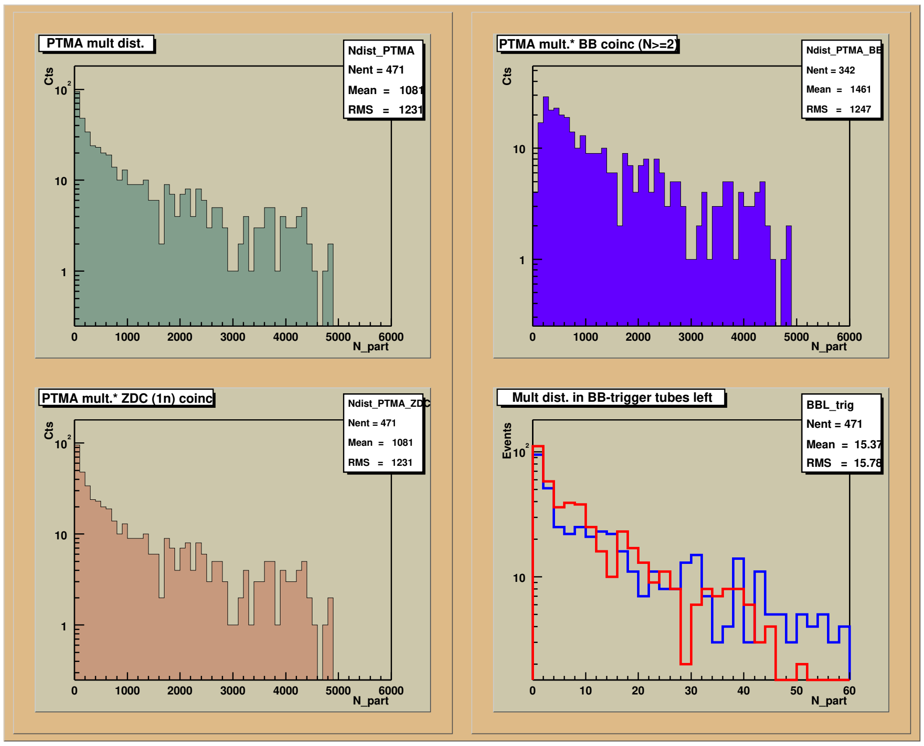

Figur 4: Nexus calculation for 130AGev (b=0-15fm) as input. The figure shows the unbiased multiplicity distribution in the PTMA array (upper left) for charged particles, the PTMA4 multiplicity distribution in coincidence with the $ZDCL(1n) * ZDCR(1n)$ requirement (lower left) and with the BB counters requiring $(N >= 2)$ in each array of big tubes. Lower right panel shows distribution of hits in each BB array. Note that the BB trigger introduces a significant bias in the selection of events, while the ZDC does not.

2.2 Particles from background.

In these simulations nothing is known about background particles, nor secondaries. This can however be investigated in GEANT by comparing calculations that allow the production of secondary particles in the material surrounding the detectors with calculations for which such interactions are turned off.

From such a comparison the fraction of extra particles produced in by secondary interactions can be estimated and the total measured multiplicity can be corrected. Of particular interest is the comparison of the dE and Etot spectra obtained in these two modes. This will reveal if the energy deposition pattern (i.e. the dE spectra) for the secondaries is significantly different from that of the primaries.

If this is not the case, the experimentally determined number of particles

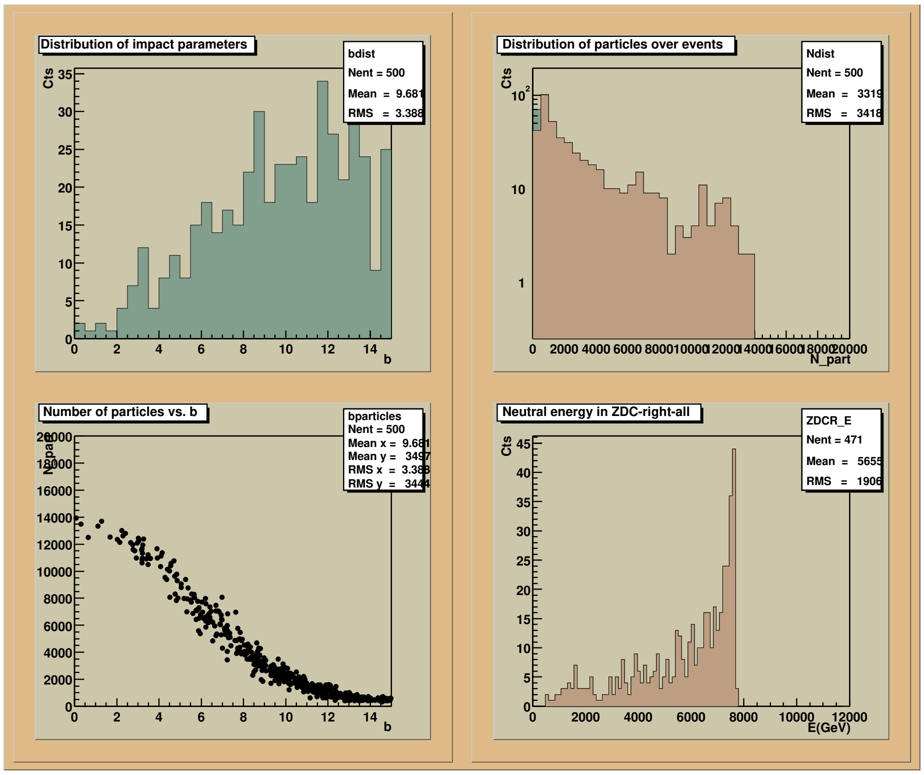

Figur 5: Nexus calculation for 130AGev (b=0-15fm) as input. The figure shows the total distribution of impact parameters (upper left), total distribution of produced particles vs b (lower left), the unbiased multiplicity distribution in the PTMA array(upper left) for all particles and the neutral energy spectrum in one ZDC (lower right)

should just be rescaled by the fraction of number of secondaries to total number of particles.

If it is very different, then the estimated average energy per additional secondary particle must be determined by subtracting the two dE/dx distributions resulting from calculation with and without production of secondaries.

The number of primaries in each event can then be calculated from

$$Nprimary = (Etot - Nsecondary* < Esecondary >)/ < Eprimary >$$

Presumably the total number of secondaries increases with increasing pseudorapidity while the importance of the high energy tail in the energy loss spectra diminishes. In any case, we should carefully consider the effect of applying an upper edge cut on the measured spectrum of Etot, also in the presence of a background of secondary particles.

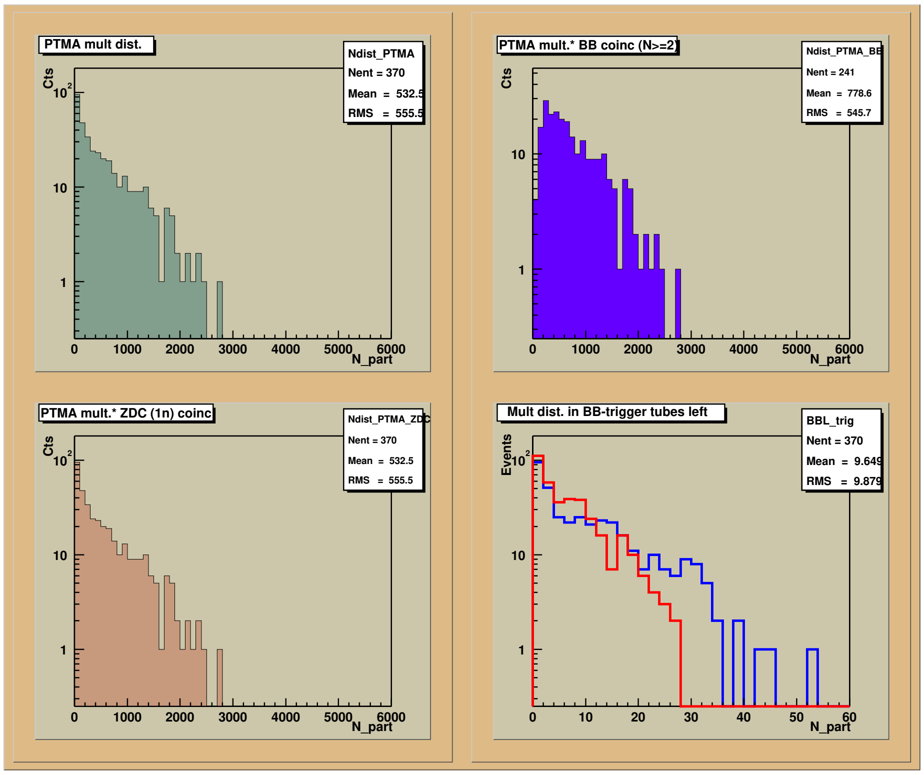

Figur 6: Nexus calculation for 130AGev (b=6.8-15fm) as input. This corresponds to approximately the most peripheral 75 % of the geometric cross section. The figure shows the unbiased multiplicity distribution in the PTMA array(upper left) for charged particles, the PTMA4 multiplicity distribution in coincidence with the $ZDCL(1n)xZDCR(1n)$ requirement (lower left) and with the BB counters requiring $(N >= 2)$ in each array of big tubes. Lower right panel shows distribution of hits in each BB array.

Erik Jacobsen is right now looking at the output of GEANT simulations for the PTMA and carrying out an analysis similar to the present one. A new note will follow up on this soon.

3 Charged particle pseudorapidity distributions from NEXUS and HIJING.

As a final item we include some results for the total charged particle multiplicity (defined as all pions, kaons and protons of either sign). As is well known NEXUS overpredicts the data by a factor of almost 2, while HIJING is more or less in the right ballpark.

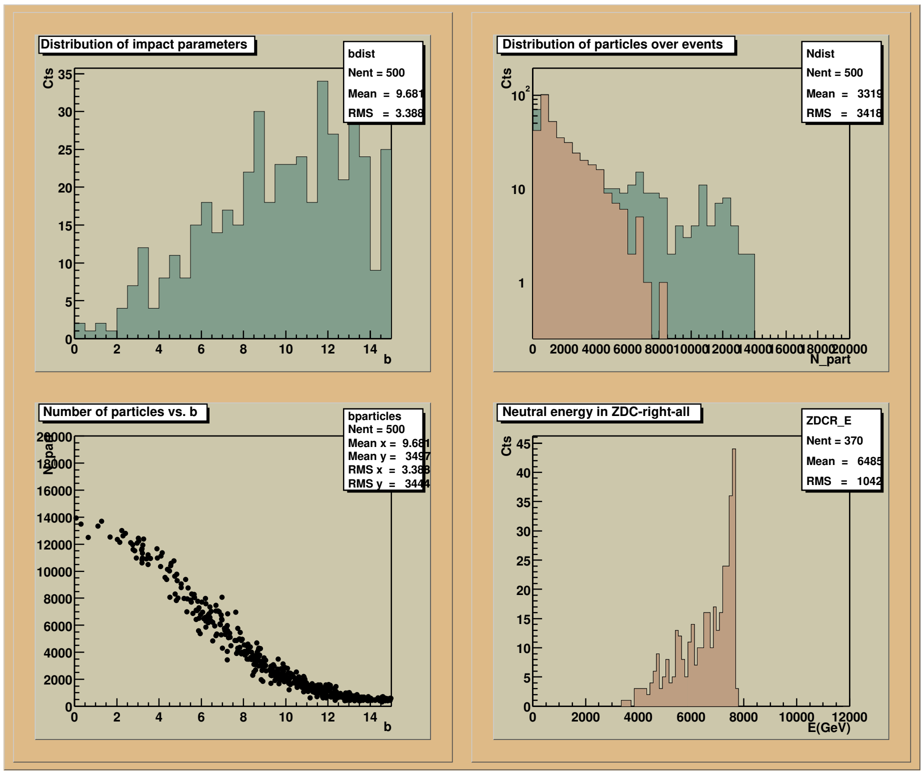

Figur 7: Nexus calculation for 130AGev (b=6.8-15fm) as input. The figure shows the total distribution of impact parameters, the total distribution of produced particles vs b, the unbiased multiplicity distribution in the PTMA array(upper left) for all particles and the neutral energy spectrum in one ZDC with the actual b cut.

One notes that HIJING shows a dip in the dN/deta distribution at eta=0. By comparing to pp. 205 ff in the QM99 proceedings, one sees that this behaviour depends on the details of the calculation. In particular including some parton shadowing effects and some jet quenching the dip can be made to disappear. Also there are other input parameters that can affect the total number of particles.

We should probably take a closer look at the options in HIJING. Does anybody have experience with this?

4 Conclusions.

The main conclusion to be drawn here is that the calculation of particle multiplicities depends significantly on model simulations of the energy loss of the produced particles in the detector segments. This is, however, a problem involv-

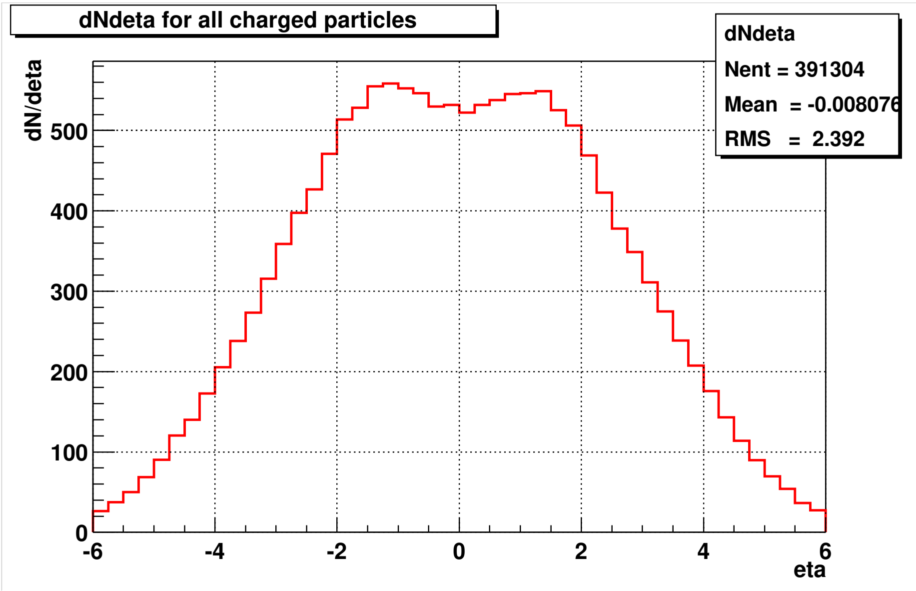

Figur 8: Hijing calculation at 130GeVA, b=5fm, for pion, kaons, p of both signs.

ing well known physical processes and should not scare us.

It also turns out that the dependence of total energy loss distributions on the particle distributions predicted by different models (e.g. HIJING and NEXUS) is quite weak. The average of the energy loss spectra varies less than 5% for the different calculations considered. We find that calculating the number of particles by the total energy deposited in an event by the average of the energy loss spectrum reproduces the 'actual' number of particles within 2-3 % with distribution widths (FWHM) of typically less than 10 % in the case of tiles close to midrapidity (PTMA4), and within 1% with widths of less than 5%, for tiles at the largest pseudorapidities (PTMA1) .

The systematic errors decrease as we move away from midrapidity and are about a factor of two smaller for PTMA1 as compared to PTMA4. This should be exploited in the presentation of results.

The dependence on collision centrality is also found to be weak and within the quoted 5%. Thus we should be able to use similar analysis methods for spectra defined to different centrality intervals.

As a further source of comfort we find that the error made in determining particle multiplicities is directly proportional to the value of the used average particle energy loss, as we would expect. Thus we either 1) use an experimental value for the energy loss of (close to MIP) particles from lab. tests and rescale this to the calculated average energy loss of the real mix of particles or 2) determine experimentally the average energy loss from single particles in the reaction or 3) use the value for the average dE per particle from simulations.

Method 2 is obviously the best, but 3 is not bad either. Method 1 is really equivalent to method 3 as it relies on simulating spectra and energy losses.

Thus, we conclude that the contribution to systematic errors from varying assumptions of the underlying physics is small and in the range 5-10%.

Further corrections arise when we determine the contribution of background particles (i.e. secondaries). We would nevertheless expect the production of secondaries to be proportional to the number of primaries. Since the pattern of energy deposition of primaries varies little we are led to predict that the pattern of energy deposition of secondaries varies correspondingly little from model to model.

It is not clear whether one should apply any cut on Etot. It is certainly not motivated as long as we only consider the primary particles. Our feeling at the moment is that we probably should not do so, even when we consider the background particles unless we firmly understand the influence of such a cut. Eq. 4 can be used to calculate the particle multiplicities using the results of simulations in a well determined fashion.

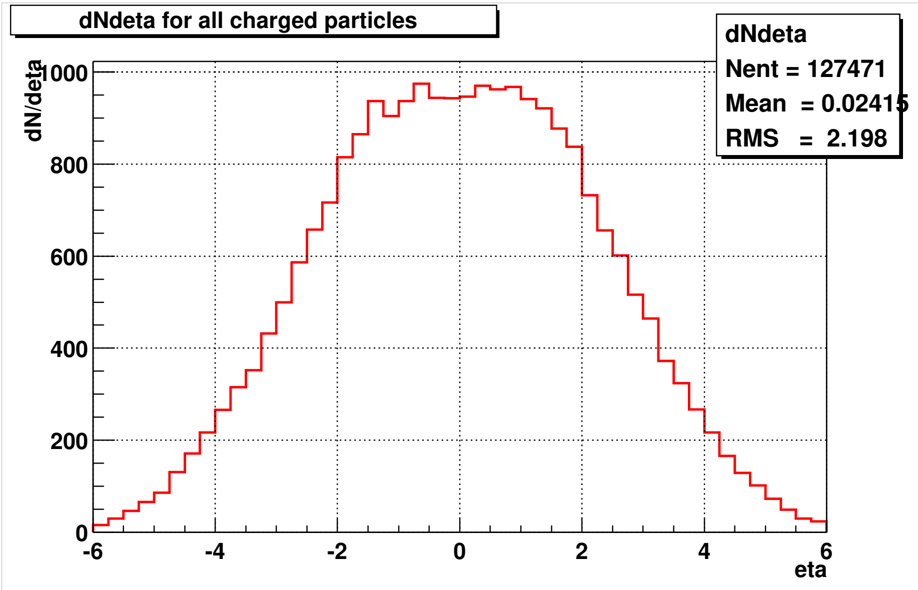

Figur 9: Nexus calculation at 130GeV.A, b=0-3.5fm for pion, kaons, p of both signs, approx 5% of total geometric cross scetion.

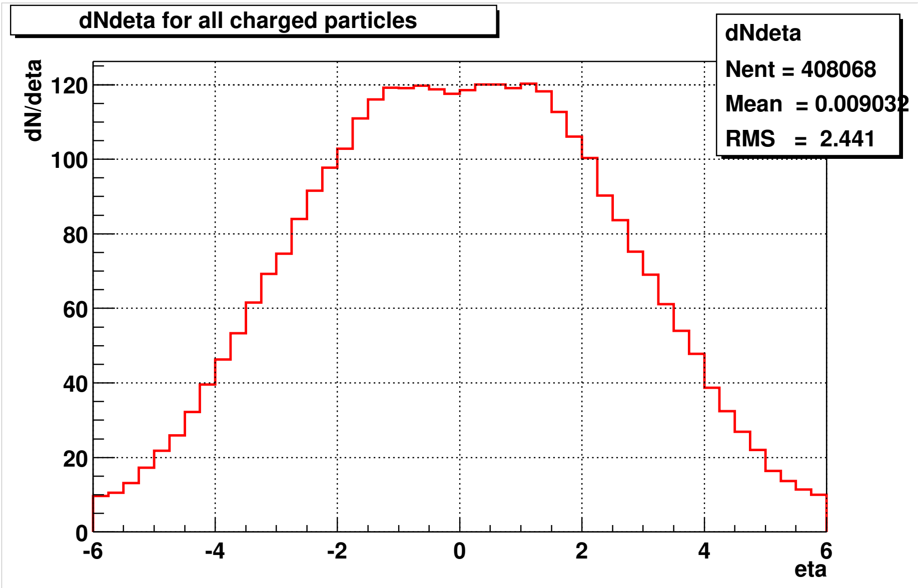

Figur 10: Nexus calculation at 130GeV.A, b=6.8-15fm for pion, kaons, p of both signs. This corresponds to the most peripheral 74 percent of the geometric cross section.

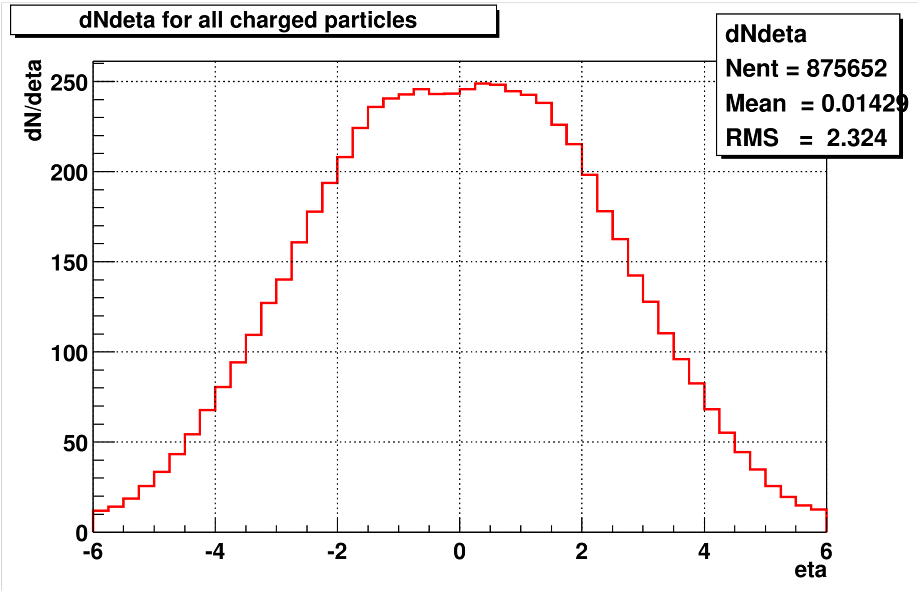

Figur 11: Nexus calculation at 130GeV.A, b=0-15fm for pion, kaons, p of both signs.